

# K-R CURVES OF THIN 2195-T8 ALUMINIUM ALLOY PLATE

R. Doglione, D. Firrao

Politecnico di Torino, Italy, C.so Duca degli Abruzzi 24, 10129 Torino, Italy, phone -39-011-5644612, fax -39-011-5644699, e-mail doglione@athena.polito.it

## ABSTRACT

The dependence of the raising toughness (R-curves) of a 2195-T8 Al-Cu-Li alloy plate on the microstructure is studied. Large intermetallic particles organised in arrays along the rolling direction serve as nucleation sites of ductile fracture; crack growth occurs mainly by pop-in. The application of Rice and Johnson's criterion for ductile fracture, making appropriate use of the average inclusion spacing along the fracture path in LT and TL direction, leads to satisfactory predictions of the onset of pop-ins and of the R-curves toughness plateaus.

## KEYWORDS

Al-Cu-Li-Mg-Zr Plate, K-R Curve, Pop-in, Inclusions.

## INTRODUCTION

Among Al-Li alloys, the Weldalite family (Al-Cu-Li-Mg-Ag-Zr) was developed to achieve high strength in the stretched and artificially aged (T8), artificially aged (T6) and naturally aged (T3 and T4) conditions [1]. Compared to other Al alloys, they have a much greater response to natural ageing, as well as being able to achieve high strength and adequate ductility after artificial ageing [2]. The Weldalite alloys are then used in welded structures [3], where a T6 treatment after welding is almost impossible, and in forgings [4], where non uniform stretching could result in undesirable variations in mechanical properties.

The first developed alloy, 2095 (Cu 4.75, Li 1.26, Mg 0.38, Ag 0.38, Zr 0.1 wt. pct.), was characterised in the T8 temper by extremely high tensile strength, often exceeding 700 MPa, but by a rather low fracture toughness, of the order of 20 MPa $\sqrt{m}$  [2]. Alloy 2195 was then developed, with the aim of excellent fracture toughness/strength combinations. To the purpose, both Cu and Li content were lowered, and by T8 temper it was possible to reach a strength exceeding 600 MPa, as well as a fracture toughness of the order of 30 MPa $\sqrt{m}$  or more.

Nowadays, tensile characteristics of rolled, forged and extruded 2195 alloy in the T8 temper are known. On the other hand, fracture toughness  $K_{Ic}$  has been reported till now for nominal plane strain conditions, which are appropriate only for thick components; fracture toughness determination for thin plates is actually lacking, mainly because of peculiar R-curve behaviour of thin products. Besides, in damage tolerant applications, the  $K_{Ic}$  value is unable to describe the full spreading of the material toughness. In these cases, the K-R curve is the only suitable approach; yet, K-R curves determinations have been scarce for Al-Li alloys, with very few reported data only for 2090 and 8090 alloys [5-13].

Suitable correlations between fracture mechanisms and R-curves, as well as the explanation of the curve on the basis of microstructural parameters have also to be sought. This point is extremely important, because only a thorough knowledge of the influence of the microstructure on the toughness may lead to the optimization process (through chemical composition variations and temper modifications) of the alloys. In order to clarify the problem, it was decided to study the K-R curve behaviour of a 6.35 mm thick 2195-T8 alloy plate and the intervening fracture mechanisms.

## EXPERIMENTAL

2195-T8 alloy was received by Reynolds in the form of 6.35 mm thick plate. Details on the chemical composition are given in Table 1. Tension tests were performed in both L and LT directions under strain control at strain rates of  $10^{-4} \text{ s}^{-1}$ . The average results are reported in Table 2.

TABLE 1  
CHEMICAL COMPOSITION OF THE ALLOY (WEIGHT %).

Cu	Li	Mg	Ag	Zr	Si	Fe	Mn	Al
3.94	0.95	0.37	0.39	0.13	0.02	0.03	0.002	bal.

Fracture mechanics tests were performed on C(T) samples 26 mm wide, in the LT and TL crack plane orientations. The single specimen method coupled with the secant reciprocal slope technique was employed, according to the ASTM E561-92 Standard. The tests were performed in crack opening displacement control. It yields decreasing crack growth driving forces, which allow to follow a ductile fracture process entirely, thus limiting the effects of pop-ins and the possibility of global instability.

The microstructure was analyzed by optical microscopy on metallographic samples. Finally, the failure mechanism were studied by microfractographic observations on the fracture surfaces by a Scanning Electron Microscope.

## RESULTS

As expected, tensile properties (Table 2) are very high and particularly attractive. A certain anisotropy between L and LT directions is evidenced, pointing out to the presence of crystallographic textures induced by the plate rolling schedule and its subsequent solubilisation treatment. Finally, the strain hardening capabilities are expressed in terms of the Hollomon law in Table 2; owing to the high strength of the alloy, the hardening exponent  $n$  is very low, as expected.

With regard to fracture mechanics tests, load-displacement data indicate a classical high strength Al alloy behaviour, i.e. frequent and at times large pop-in steps. Nevertheless, 2195-T8 alloy shows a globally stable behaviour, being possible to control the fracture process along the decreasing part of the load-crack opening displacement diagram. This produced stepped K-R curves, Figure 1.

TABLE 2  
TENSILE PROPERTIES OF 2195-T8 ALLOY.

direction	E [GPa]	Re [MPa]	R [MPa]	A%	n	k [MPa]
L	72.8	580	602	8.5	0.022	668
LT	72.6	548	578	10	0.035	682

The microstructure, typical of many high strength aluminium alloys, is made of coarse (several millimeters long) unrecrystallised columnar grains mixed with fine nearly equiaxed recrystallised grains (10  $\mu\text{m}$  ca. diameter). These appear to be located at the boundaries of the large columnar grains, or inside them, when there is a local high concentration of intermetallic particles. These particles are mainly arranged in rows following the rolling direction. The average interparticle spacing inside each inclusion array is of the order of 30  $\mu\text{m}$ , whereas in the long transverse direction the inclusions rows are on the average 480  $\mu\text{m}$  apart.

The fracture mechanism is ductile, mainly transgranular, even if some intergranular character is present. The dimples are developed around the previously cited intermetallics. The cavities are nearly equiaxed around the coarser particles, whereas smaller intermetallics give rise to dimples elongated in the crack growth direction because they encompass several particles. Very elongated dimples are more pronounced and frequent in TL samples.

## DISCUSSION

The K-R curves reported in Figure 1 show some peculiar characteristics, namely the grouped distribution of points spaced by pop-ins more visible in the upper part of the curves. Here, after pop-in and crack arrest, new low elevation high K level blunting occurs.

In order to explain the differences in the R-curves and the presence of an approximative toughness plateau in the TL direction, it is necessary to take into account the inclusion distribution, as detailed in the previous paragraph and that, as here reported, fracture is predominantly ductile, by nucleation, growth and coalescence of voids around biggest second phases particles.

Toughness in the TL direction is then related to the inclusion spacing along inclusions rows produced by rolling of the plate. Assuming the validity of the classical fracture criterion proposed by Rice and Johnson [14], critical conditions for fracture are reached when the heavily strained process zone (contained in the plastic zone ahead the crack tip), which scales with the CTOD, reaches the center-to-center spacing  $\lambda$  between bigger intermetallics. This prompted Hahn and Rosenfield [15] to propose a model for the attainment of ductile fracture instability in high strength aluminium alloys:

$$K_{\text{crit}} = \sqrt{2 \cdot R_e \cdot E \cdot \lambda} \quad (1)$$

The validity of this model has been questioned by Garret and Knott [16] because it predicts increasing toughness with increasing yield strength, contrary to experiments. However, the same authors recognise that the model correctly reproduces the dependence between toughness and microstructural parameters for peak aged high strength aluminium alloys..

In the present case, being the specimens not in fully plane strain because of insufficient thickness, it is necessary to substitute the factor 2 in equation 1 with a constant k, slightly greater than 2, which accounts for a mixed plane strain-plane stress state. Moreover, the initial part of the R-curve simply represents the enlargement of the plastic zone, without physical crack propagation, what corresponds to the evolution of the stress state from plane strain (at the beginning) to a more relaxed triaxiality. Modified equation 1 should then be correctly interpreted as a condition for the instability at different triaxiality levels, which are represented by different k values. Since  $R_e$ , E (Table 2) and  $\lambda$  (30 $\mu$ , see preceding paragraph) are constant, in a near plane strain state  $k \approx 2$  and modified equation 1 predict the onset of the instabilities on the R curve nearly at 49  $\text{MPa}\sqrt{\text{m}}$ , in quite good agreement with the fact that the first significant pop-ins are found on the R-curves (in the TL case) above 40  $\text{MPa}\sqrt{\text{m}}$  (Fig. 1).

Obviously, the instability is not catastrophic, because tests were conducted under crack opening control and the fracture mechanism is invariant. After crack arrest, further loading produces further stress triaxiality relaxation, an increase of the value of k above 2, and the next instability at K levels above the previous one. The R-curve may then, in average, continue to rise, but only slightly, because with progressive triaxiality

relaxation the increments of  $k$  values are small, whereas the short  $30\ \mu\text{m}$  inclusion spacing along rows in the L direction dictates the limits of the process zone, and then limits an approximative plateau of the R-curve slightly above  $50\ \text{MPa}\sqrt{\text{m}}$ .

As it regards LT specimens, the previous arguments may be valid to predict the first significant instabilities. At the beginning of loading, in a near plane strain state, some parts of the crack front are located in correspondence with an intermetallic group, where interparticle spacing is still of the order of  $30\ \mu\text{m}$ . Again following Hahn and Rosenfield, the onset of the pop-ins may be predicted to lie between  $40$  and  $50\ \text{MPa}\sqrt{\text{m}}$ , as actually verified on the R curves, e.g. Figure 1. But now the toughness plateau is not easily reached, because after a first momentary unstable crack propagation through the inclusion group, the crack front, in that region of the sample, after arrest will find the next inclusion array at a distance somewhat less (it depends on the arrest distance beyond the first inclusions) than the intermetallics row spacing,  $480\ \mu\text{m}$ ; such a distance is an order of magnitude larger than the interparticle spacing within the row,  $30\ \mu\text{m}$ .

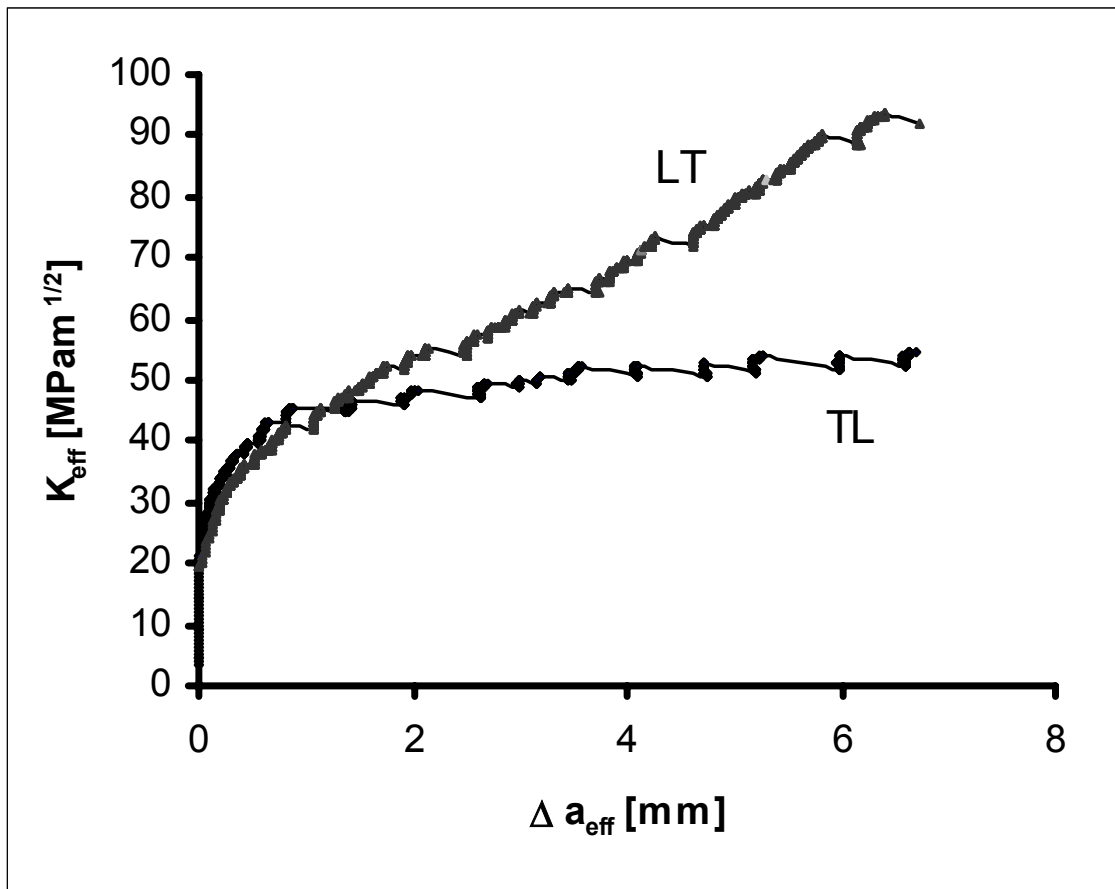


Figure 1:  $K_{\text{eff}} - \Delta a_{\text{eff}}$  curves for 2195-T8 alloy tested in the TL and LT directions.

Thus, after arrest, new instability conditions are not soon reached in the same region of the sample, and probably critical conditions may be reached easier in another region, where the crack front is closer to the next intermetallics array. The situation corresponds then to an intermittent activation of local instabilities mixed with a progressive loss of constraint and plastic zone enlargement. This explains the long rising of the R curve, and the delay in the attainment of a toughness plateau, which is not reached with the small samples utilised in the present investigation.

However, again equation 1 allows a rough estimate of the order of magnitude of the toughness plateau in the LT direction. Since the average magnitude of crack growth during pop-in in the high part of the R curve is of the order of  $230\ \mu\text{m}$ , this means that, in average, the next intermetallics array is at least about  $250$  from the actual crack front. Again invoking the Rice and Johnson's criterion, and making use of equation 1,

considering that now the sample is far from plane strain conditions, the constant  $k$  is above two and the predicted toughness plateau is above 70-80 MPa $\sqrt{m}$ , in good agreement with experimental data, Figure 1.

## CONCLUSIONS

Fracture resistance of the Al-Cu-Li-Mg-Zr 2195-T8 6 mm thick plate has been studied following the K-R curve approach. It has been found that 2195-T8 possesses excellent toughness, and this strongly related to the average inclusion spacing. Such parameter induces an important toughness anisotropy between LT and TL directions, the latter being characterised by less attractive performances. It may be concluded that a substantial reduction of the inclusions content, i.e. the coarse intermetallics, might enhance TL fracture toughness because it increases the interparticle spacing, thus postponing the attainment of critical conditions at the crack tip.

## ACKNOWLEDGEMENTS

The financial support of Agenzia Spaziale Italiana through the contract no. J97FDA1 is here acknowledged.

## REFERENCES

1. Pickens J. R., Heubaum F. H, Langan T. J. and Kramer L. S., (1989) In: *Aluminium-Lithium Alloys*, Proc. 5th Int. Aluminium-Lithium Conf., pp. 1397-1414, Sanders T. H. and Starke E. A. eds., MCEP.
2. Edwards M. R., Moore A. and Mustey A. J., (1994) In: *Aluminium Alloys*, Proc. 4th Int. Conf. Aluminium Alloys (ICAA4), Vol. II, pp. 334-341, Sanders T. H. and Starke E. A. eds., Georgia Institute of Technology,.
3. Cross C. E., Loechel L. W. and Braun G. F., (1992) In: *Aluminium-Lithium Alloys*, Proc. 6th Int. Aluminium-Lithium Conf., pp. 1165-1170, Peters M. and Winkler P. J. eds., DGM.
4. McNamara D. K., Pickens J. R. and Heubaum F. H., (1992) In: *Aluminium-Lithium Alloys*, Proc. 6th Int. Aluminium-Lithium Conf., pp. 921-926, Peters M. and Winkler P. J. eds., DGM.
5. Venkateswara Rao K. T. and Ritchie R. O., (1989) In: *Aluminium-Lithium Alloys*, Proc. 5th Int. Aluminium-Lithium Conf., pp. 1501-1512, Sanders T. H. and Starke E. A. eds., MCEP.
6. Barbaux Y., (1989) In: *New Light Alloys*, pp. 8-1, 8-18, AGARD n. 444.
7. Hart G.J., Schra L., McDarmaid D.S. and Peters M., (1989) In: *New Light Alloys*, pp. 5-1, 5-17, AGARD n. 444.
8. Doglione R., Ilia E., Firrao D., (1991) Proc. VII Conv. Naz. Gruppo Italiano Frattura, pp. 57-73, Reale S. ed., Firenze, Italy.
9. R.J.H. Wanhill, L. Schra and W.G.J. Hart, (1992) In: *Aluminium-Lithium Alloys*, Proc. 6th Int. Aluminium-Lithium Conf., pp. 253-258, Peters M. and Winkler P. J. eds., DGM.
10. Doglione R., Ilia E., Marcelli A., Firrao D., (1992), In: *Materials Development in Rail, Tire, Wing, Hull Transportation*, Vol. 1, pp. 191-200, Associazione Italiana di Metallurgia, Milano, Italy.
11. Firrao D., Doglione R., Ilia E., (1993) In: *Constraint effect in Fracture*, pp. 289-305, Hackett E. M., Schwalbe K.-H. and Dodds R. H. eds., ASTM STP 1171.
12. Doglione R., Ilia E., Firrao D., (1994) In: *Aluminium Alloys*, Proc. 4th Int. Conf. Aluminium Alloys (ICAA4), Vol. II, pp. 374-381, Sanders T. H. and Starke E. A. eds., Georgia Institute of Technology,.
13. Doglione R., Arena F., Firrao D., (1997) In: *Advances in Fracture Research*, Proc. 9th Int. Cong. Fracture, Vol. 1, pp. 259-265, Karihaloo B. L., May Y-W., Ripley M. I. and Ritchie editors R. O., Pergamon Press.
14. Rice J. R. and Johnson M. A., (1970) In: *Inelastic Behaviour of Materials*, pp. 641-672, Kanninen M. F., Adler W. F., Rosenfield A. R. and Jaffee R. I. eds., McGraw Hill.
15. Hahn G. T. and Rosenfield A.R., (1975) *Metallurgical Transactions A*, Vol. 6A, pp. 653-670.  
Garret G. G. and Knott J. F., (1978) *Metallurgical Transactions A*, Vol. 9A, 1978, pp. 1187-1201.